This full text paper was peer reviewed at the direction of IEEE Communications Society subject matter experts for publication in the IEEE ICC 2009 proceedings

A simple near-capacity bandwidth-efficient coded modulation scheme in Rayleigh fading

Nghi H. Tran, *Member, IEEE*, Tho Le-Ngoc, *Fellow, IEEE*, and Tad Mastumoto *Senior Member, IEEE*

***Abstract*— This paper proposes a near-capacity yet simple bit-interleaved coded modulation with iterative decoding (BICM-ID) scheme by employing a multi-dimensional (multi-D) mapping technique in a multi-D constellation carved from a rotated lattice. Using extrinsic information transfer (EXIT) charts, it is shown that the proposed technique fits well with simple convolutional codes in terms of the area property, for which turbo pinch-off can happen at a low E_b/N_0 value. In particular, both EXIT chart analysis and simulation results indicate that by using just a simple convolutional code together with a 4-D mapping, a turbo pinch-off and a bit error rate (BER) close to 10^{-6} happen at a signal-to-noise ratio (SNR) that is even lower than the BICM constraint capacity limit with a uniform input. The proposed BICM-ID scheme can be considered as an attractive alternative to other bandwidth-efficient coded modulation techniques using powerful turbo-like codes such as turbo or low-density parity-check (LDPC) codes over a Rayleigh fading channel.**

I. Introduction

Bit-interleaved coded modulation (BICM) [1] has been recognized as a powerful yet flexible coded modulation scheme over a Rayleigh fading channel. Information-theoretic analysis in [2] shows that BICM capacity with a uniform input and Gray mapping is almost identical to that of any coded modulation scheme and can achieve near Shannon limit. Various practical BICM-based designs have been proposed using state-of-the-art codes such as turbo-codes and turbo-like codes including LDPC codes followed by Gray mapping [3]–[6]. For instance, by using turbo codes, simulation results in [3] indicate that an excellent error performance can be attained with a small gap to BICM limit.

Lately, under the body of BICM systems, considerable attention has been paid to the idea of multi-dimensional (multi-D) anti-Gray mapping where a group of coded bits is mapped simultaneously to multiple symbols of a complex 1-D constellation [7]–[9]. It was demonstrated in [7], [9] that a remarkable improvement can be achieved by using multi-D anti-Gray mapping together with a simple convolutional code. However, simulation results in [9] show that the performance of a classical BICM system using turbo codes and Gray mapping still outperforms that of the multi-D mapping system. This is consistent with the information-theoretic considerations presented in [2], where it is proven that with the same 1-D signal points transmitted, anti-Gray mapping is suboptimal. To the best of our knowledge, up to date, the combination of a turbo-like code and Gray-like mapping under a BICM framework is the most powerful method for achieving near-capacity over Rayleigh fading channels.

Signal space diversity (SSD) with full-diversity rotation [10]–[12] has been recently considered as an effective technique for increasing diversity order over a fading channel. By applying SSD at a sufficiently high-dimensional signal space, e.g., 32-D, it was shown in [10], [12] that the error performance over a Rayleigh fading channel asymptotically approaches that over an AWGN channel for both uncoded and coded systems. However, the results in [10], [12] hold only when the system operates at a sufficiently high signal-to-noise ratio (SNR). Consequently, the performance of SSD systems in [10], [12] is still far from the capacity limit.

Observe that the diversity benefit offered by SSD has been extensively investigated in the literature. However, the other important advantage of SSD in providing larger mutual information between the input and output of the channels [13] has received little attention. This paper shall exploit this benefit to propose a simple BICM with iterative decoding (BICM-ID) scheme to overcome the disadvantage of the previous multi-D mapping system over a Rayleigh fading channel. In particular, by using extrinsic information transfer (EXIT) charts [14], it is shown that performing a multi-dimensional mapping over a multi-dimensional constellation carved from a rotated lattice in only a reasonably low dimensional signal space together with a simple convolutional code is an excellent combination and near-capacity performance can be attained. Both EXIT chart analysis and simulation results indicate that a turbo pinch-off resulting in a bit error rate (BER) close to 10^{-6} happens at an SNR that is even lower than BICM capacity limit by using just a simple convolutional code together with a 4-D mapping. It means that the proposed scheme outperforms any classical BICM systems using turbo-like codes.

II. System Model

The block diagram of the proposed BICM-ID system is depicted in Fig. 1. First, a suitable convolution encoder that shall be determined later encodes binary information sequence $\boldsymbol{u}$ into a coded sequence $\boldsymbol{c}$. After being interleaved, multi-D mapping technique is employed by mapping simultaneously Nm coded bits to a sequence of N 1-D symbols $\boldsymbol{s} = [s_1, s_2, \ldots, s_N]^\top$ using a mapping rule ξ, where each symbol s_i is in a conventional 1-D constellation Ω, such as QAM, of

This work was supported in parts by the Natural Sciences and Engineering Research Council of Canada (NSERC), and by the Japanese government funding program, Grant-in-Aid for Scientific Research (B), No. 20360168.

Nghi H. Tran and Tho Le-Ngoc are with the Department of Electrical & Computer Engineering, McGill University, Montreal, Quebec, Canada. Email: nghi.tran@mcgill.ca, tho@ece.mcgill.ca.

Tad Mastumoto is with Japan Advanced Institute of Science and Technology, Japan, and Center for Wireless Communication at University of Oulu, Finland. Email: matumoto@jaist.ac.jp.

978-1-4244-3435-0/09/$25.00 ©2009 IEEE

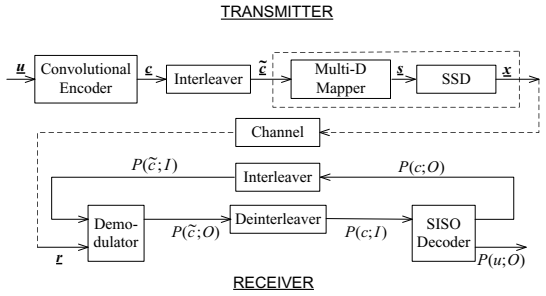

Fig. 1. The proposed BICM-ID system with multi-D mapping and SSD.

size 2^m. The super symbol $\boldsymbol{s}$ is considered to be in an N-D constellation Ψ of size 2^{Nm}. By using SSD, the symbol $\boldsymbol{s}$ is rotated by an $N \times N$ rotation matrix $\boldsymbol{G}$ to obtain the rotated symbol $\boldsymbol{x} = [x_1, x_2, \ldots, x_N]^\top$ as $\boldsymbol{x} = \boldsymbol{G}\boldsymbol{s}$. In this work, it is of our interest to consider a full-diversity rotation for which $\boldsymbol{x} - \boldsymbol{y} = \boldsymbol{G}(\boldsymbol{s} - \boldsymbol{p})$ contains all nonzero components as long as $\boldsymbol{s} \neq \boldsymbol{p}$, $\boldsymbol{s}$ and $\boldsymbol{p}$ in $\boldsymbol{\Psi}$. The reason that we pay attention to this rotation is because the full-diversity rotation can increase the mutual information over a Rayleigh fading channel [13]. As shown later, one can reap a tremendous benefit with this improvement when designing an outer convolutional code and multi-D mapping by EXIT charts.

Consider a fully-interleaved flat Rayleigh fading channel, where the channel changes independently in each component duration of the N-dim signal symbol, with full channel state information (CSI) available at the receiver but not the transmitter. The N-D received signal $\boldsymbol{r}$ is given as:

$$\boldsymbol{r} = \boldsymbol{H}\boldsymbol{G}\boldsymbol{s} + \boldsymbol{w}. \tag{1}$$

In (1), the matrix $\boldsymbol{H} = \mathrm{diag}(h_1, \ldots, h_N)$ contains the fading coefficients in its diagonal, where each diagonal element h_i is $\mathcal{CN}(0,1)$[1]. Each element w_i of white Gaussian noise $\boldsymbol{w} = [w_1, \ldots, w_N]$ is $\mathcal{CN}(0, N_0)$.

The receiver of the proposed system includes the soft-input soft-output (SISO) demodulator and the SISO channel decoder as shown in Fig. 1. The optimal demodulator, i.e., the maximum a posteriori probability (MAP) demodulator [4], is implemented in N-D signal space as long as either multi-D mapping ξ or SSD is used. Therefore, the proposed system has the same receiver complexity as that of multi-D mapping systems presented in [7]. The SISO channel decoder uses the MAP algorithm in [15]. There is an iterative processing between the demodulator and the channel decoder to exchange the extrinsic information of the coded bits.

III. Design using EXIT Charts

With the assumption of error-free feedback, Appendix I analyzes the asymptotic union bound on the BER performance of the proposed system for the completeness of the paper. The derived bound can be used to accurately predict the asymptotic BER performance without the need of running time-consuming simulations. However, the analytical technique presented in Appendix I is only useful to predict the error performance of an iterative demodulation and decoding scheme at the BER floor region. What is of more interest is a so-called turbo pinch-off, or water-fall, region, where a significant BER reduction is observed over iterations. The turbo pinch-off region can be used to examine whether the iterative demodulation and decoding system under consideration can achieve near-capacity performance (please see [16] and references therein).

This section analyzes the convergence property of the proposed system in the turbo pinch-off region for a close-capacity performance using EXIT chart [14]. Following the same notations as in [14], let I_{A1} and I_{E1} denote the mutual information between the *a priori* LLR and the transmitted coded bit, and between extrinsic LLR and the transmitted coded bit at the input and output of the demodulator, respectively. Similarly, I_{E2} and I_{A2} are the mutual information representing the *a priori* knowledge and the extrinsic information of the coded bits at the input and output of the decoder.

In the following, the advantage offered by SSD is first demonstrated with the aid of EXIT curves for the demodulator. Then a combination of multi-D demodulator and a simple convolutional decoder, with which close-capacity performance can be achieved, is proposed by matching demodulator EXIT curve to decoder EXIT curve. For simplicity, we only consider QPSK constellation, together with a rate 1/2 convolutional code. For comparison, BICM capacity limit computed with a uniform input, Gray mapping, and a rate $1/2$ code [2] is considered as a benchmark. This is a fair criterion, since the parameter sets the limit for the most effective coded modulation scheme up to the present time as discussed earlier. Furthermore, multi-D anti-Gray mapping proposed in [7] that minimizes $\delta(\boldsymbol{\Psi}, \xi, \boldsymbol{G})$ in (7) when $\boldsymbol{G} = \boldsymbol{I}_N$ is of our main interest. Note that other anti-Gray mapping rules can be obtained by using the compact design criterion for a given full-diversity rotation $\boldsymbol{G}$ in (9).

A. EXIT curves of multi-D demodulator with and without SSD

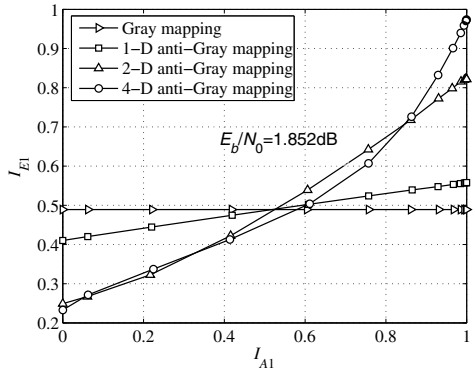

Fig. 2. Multi-D demodulator EXIT curves at E_b/N_0=1.852dB for different mapping rules without SSD.

First, consider the case without using SSD technique and the constellation Ω is QPSK. Figure 2 shows EXIT curves

[1]Here $\mathcal{CN}(0,1)$ denotes a circularly symmetric complex Gaussian random variable with variance $1/2$ per dimension.

of the demodulator for different types of mapping rule ξ at $E_b/N_0 = 1.852$dB, where E_b is the energy per information bit with code rate $r_c = 1/2$. Note that $E_b/N_0 = 1.852$dB is the BICM capacity limit computed with Gray mapping, QPSK constellation, and a rate $1/2$ code [2], [6]. These mappings include conventional Gray mapping, 1-D, 2-D, and 4-D anti-Gray mapping proposed in [7]. It can be seen from Fig. 2 that the EXIT curve with Gray mapping is completely horizontal. This makes Gray mapping a good match for powerful turbo-like codes, because EXIT curves of these codes are also almost horizontal [5]. On the other hand, EXIT curves of anti-Gray mappings exhibit steep slopes, which make them suitable for other class of codes having also decayed EXIT curve, such as convolutional codes. However, observe that the higher the dimension of multi-D mapping, the slope is steeper with a smaller starting point at $I_{A1} = 0$. As a result, the turbo pinch-off region happens at higher SNR. This is the main disadvantage of a multi-D mapping system considered in [7], since it requires a relatively high SNR at which turbo pinch-off happens. As shown in the next subsection, there does not exist any suitable outer convolutional code that makes a multi-D mapping system without SSD perform close enough to the BICM capacity limit.

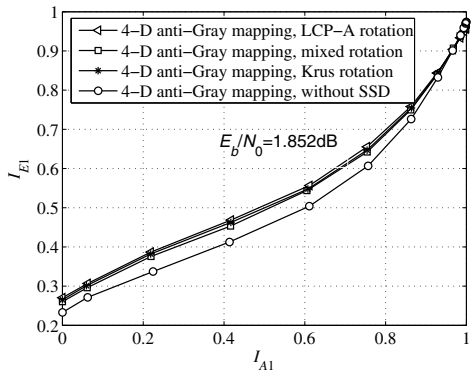

Fig. 3. 4-D demodulator EXIT curves at E_b/N_0=1.8dB for anti-Gray mapping with different rotations.

Since the area under the multi-D demodulator EXIT curve can be approximated as the mutual information between the input and output of the channel [17], one can apply the full-diversity rotation to improve the transfer characteristic of multi-D demodulator, and as a consequence, to overcome the disadvantage of the previous multi-D mapping system. Figure 3 plots EXIT curves of the demodulator using 4-D anti-Gray mapping and different rotations $\boldsymbol{G}$ of size 4 at E_b/N_0=1.852dB. The rotations include the Krus and mixed rotations given in [18], and the LCP-A rotation with $N = 4$ given in [10], [11] as

$$\boldsymbol{G} = \frac{1}{\sqrt{N}} \begin{pmatrix} 1 & \alpha_1 & \dots & \alpha_1^{N-1} \\ \vdots & \vdots & & \vdots \\ 1 & \alpha_N & \dots & \alpha_N^{N-1} \end{pmatrix}, \qquad (2)$$

where $\alpha_1 = \alpha = \exp\left(j\frac{2\pi}{2^{q+2}}\right)$ and $\alpha_i = \alpha \exp\left(j\frac{2\pi(i-1)}{2^{q+2}}\right)$. The 4-D demodulator EXIT curve employing 4-D anti-Gray mapping without rotation is also provided for comparison. It can be seen from Fig. 3 that with the same 4-D anti-Gray mapping, full-diversity rotation provides higher I_{E1} in a wide range of I_{A1}. The reason for this improvement is in the increase in the constrained capacity with a rotated constellation [13]. As we shall see, this advantage of rotation makes it a perfect match to a simple outer convolutional code. Although the LCP-A rotation is most preferred, it is clear that there is not much difference in the EXIT curves of three rotations.

B. EXIT curve matching

This subsection applies EXIT chart technique [14] to select the most suitable convolutional code for the proposed system. By using EXIT charts, both EXIT curves of the multi-D demodulator and the decoder are plotted in the same graph, but the axes of the EXIT curve of the decoder are swapped [14]. The convergence behavior of multi-D mapping system can therefore be visualized. It should be mentioned that for the system under consideration, the EXIT curve of a rate r_c convolutional code does not depend on SNR and always crosses the middle point $(0.5, r_c)$ [14].

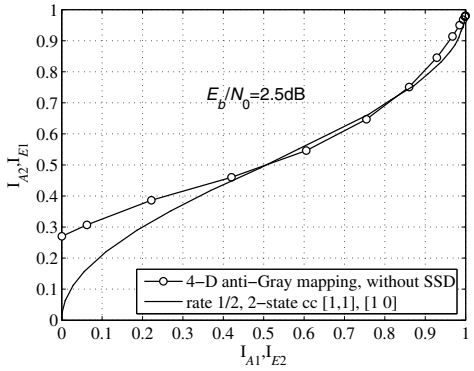

Fig. 4. EXIT charts of the 4-D demodulator using 4-D anti-Gray mapping, no SSD at E_b/N_0=2.5dB and rate 1/2, 2-state convolutional code (cc).

We first examine the EXIT charts of multi-D mapping system without using SSD. Figure 4 plots the EXIT curves of 4-D anti-Gray mapping without using SSD and a rate 1/2, 2-state convolutional code with generator polynomials $\mathbf{g}_1 = [1, 1]$ and $\mathbf{g}_2 = [1, 0]$. Note that the 2-state code is the simplest possible convolutional code. The signal to noise ratio is set at $E_b/N_0 = 2.5$dB, which is about 0.65dB from the BICM benchmark. It can be seen from Fig. 4 that the two EXIT curves quickly intersect and the intersection point falls in the lower left quadrant of the EXIT plane. Since the EXIT curve of a more powerful rate 1/2 convolutional code exhibits a sharper slope at the beginning, it is straightforward to see that no convolutional code can be matched with 4-D anti-Gray mapping in order to achieve a high extrinsic mutual information at $E_b/N_0 = 2.5$dB. This adverse behavior holds for any higher multi-D anti-Gray mapping, due to its steeper EXIT curve. In overall, it is clear that that conventional multi-D mapping technique cannot perform close to the BICM benchmark. Observe from the simulation results in [7] that

the turbo-cliff region happens at around $E_b/N_0 = 3$dB, which is 1.15dB away from the BICM benchmark. This result is expected, since by using the same QPSK signal points to carry coded bits, Gray mapping is preferred with respect to the information-theoretic analysis [2].

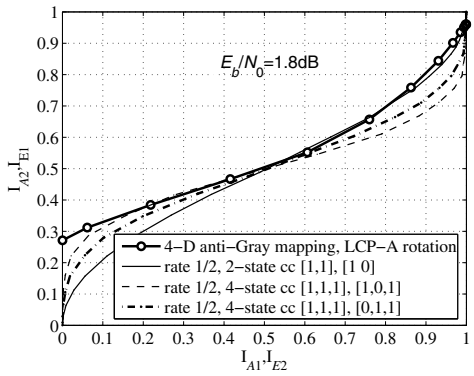

Fig. 5. EXIT charts of the 4-D demodulator using 4-D anti-Gray mapping, LCP-A rotation at E_b/N_0=1.8dB, and rate 1/2, 2-state cc with $\mathbf{g}_1 = [1, 1]$ and $\mathbf{g}_2 = [1, 0]$, 4-state cc with $\mathbf{g}_1 = [1, 1, 1]$ and $\mathbf{g}_2 = [1, 0, 1]$, and 4-state cc with $\mathbf{g}_1 = [1, 1, 1]$ and $\mathbf{g}_2 = [0, 1, 1]$.

Now consider the case when SSD is applied. Figure 5 plots the EXIT curve of 4-D anti-Gray mapping using LCP-A rotation at E_b/N_0=1.8dB, which is smaller than the BICM benchmark, and the EXIT curves for various rate 1/2 convolutional codes. Besides the rate 1/2, 2-state convolutional code given earlier and the standard rate 1/2, 4-state convolutional code with generator polynomials $\mathbf{g}_1 = [1, 1, 1]$ and $\mathbf{g}_2 = [1, 0, 1]$, the EXIT curve of rate 1/2, 4-state convolutional code with generator polynomials $\mathbf{g}_1 = [1, 1, 1]$ and $\mathbf{g}_2 = [0, 1, 1]$ is also plotted. Note that this convolutional code has not been widely used. It can be verified that the minimum Hamming distance of this code is $d_H = 4$, as compared to $d_H = 3$ and d_H=5 of the two above standard convolutional codes.

It is clear from Fig. 5 that the EXIT curve of the standard rate 1/2, 4-state convolutional code with generator polynomials $\mathbf{g}_1 = [1, 1, 1]$ and $\mathbf{g}_2 = [1, 0, 1]$ does not fit well to the demodulator EXIT curve as similar to the previous case. This implies that more powerful convolutional codes are not suitable either. The EXIT curve of rate 1/2, 2-state code intersects the demodulator EXIT curve in the upper right quadrant of the EXIT plane, but at a low mutual information, which does not guarantee low BER. On the other hand, it is interesting to see that the EXIT curve of uncommon rate 1/2, 4-state code with generator polynomials $\mathbf{g}_1 = [1, 1, 1]$ and $\mathbf{g}_2 = [0, 1, 1]$ matches very well to the demodulator EXIT curve. The two EXIT curves do not intersect until reaching the ending point $I_{A_1}(1)$ with very high mutual information, leading to a low BER. To the best of our knowledge, this is the best match reported so far over a Rayleigh fading channel.

IV. Simulation Results

This section provides analytical and simulation results to confirm the analysis made in the previous sections and the advantage offered by the proposed system. The convolutional code is again the rate 1/2, 4-state code with generator polynomials $\mathbf{g}_1 = [1, 1, 1]$ and $\mathbf{g}_2 = [0, 1, 1]$. Furthermore, 4-D anti-Gray mapping is employed in the rotated constellation using LCP-A rotation $\boldsymbol{G}$. A random interleaver of length 3×10^5 is used. Each point in the BER curves is simulated with 6×10^6 to 6×10^8 coded bits. In the computation of the asymptotic bound for P_b in (3), the first 20 Hamming distances of the convolutional code is included.

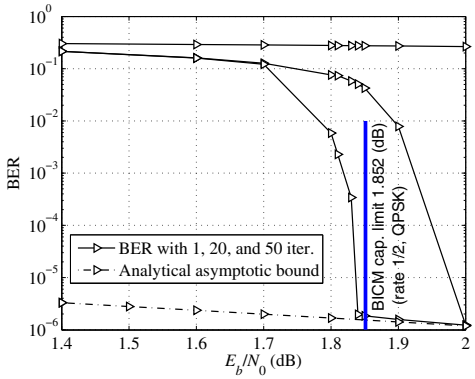

Fig. 6. BER performance of the proposed system using 4-D anti-Gray mapping and LCP-A rotation, together with a rate 1/2, 4-state cc $\mathbf{g}_1 = [1, 1, 1]$ and $\mathbf{g}_2 = [0, 1, 1]$.

Figure 6 shows the BER performance for the system under consideration with 1, 20 and 50 iterations. It can be seen from Fig. 6 that the analysis made by EXIT charts agrees with the BER curves. In particular, the turbo cliff region happens around E_b/N_0=1.8dB and one achieves a BER close to 10^{-6} with 50 iterations at E_b/N_0=1.84dB, which is even smaller than the BICM benchmark. The tightness of the asymptotic bound in the error floor area is also clearly observed, which makes it an effective tool to predict the error performance at relatively low BER regions.

V. Conclusions

This paper proposed a novel bandwidth-efficient coded modulation scheme by combining the ideas of multi-D mapping and SSD technique. Both EXIT chart analysis and simulation results showed that by only using a simple convolutional code as an outer code, the proposed scheme can outperform any classical BICM system with a uniform input and Gray-like mapping together with powerful turbo-like codes such as turbo codes or LDPC codes. The error bound on the asymptotic performance was also derived, which can be used to estimate the asymptotic performance of the proposed system in the error-floor area.

Appendix I
Tight Bound and Design Criterion on The Asymptotic Performance

Given a rate k_c/n_c convolutional code with distance spectrum $\{c_d\}$, i.e., c_d is the total information weight of all error events at Hamming distance d, the union bound on the BEP

for a BICM-ID system employing constellation $\boldsymbol{\Psi}$, mapping rule ξ and rotation $\boldsymbol{G}$ is given as:

$$P_b \leq \frac{1}{k_c} \sum_{d=d_H}^{\infty} c_d f(d, \boldsymbol{\Psi}, \xi, \boldsymbol{G}) \tag{3}$$

where d_H is the minimum Hamming distance of the convolutional code. In (3), the function $f(d, \boldsymbol{\Psi}, \xi, \boldsymbol{G})$ is the average pairwise error probability, which depends on the Hamming distance d, the constellation $\boldsymbol{\Psi}$ and the mapping ξ, as well as the rotation matrix $\boldsymbol{G}$. Let $\underline{\boldsymbol{c}}$ and $\underline{\check{\boldsymbol{c}}}$ be the input and decoded sequences with Hamming distance d between them. Furthermore, assume that $\underline{\boldsymbol{c}}$ and $\underline{\check{\boldsymbol{c}}}$ differ in the first d consecutive bits. With the use of a sufficiently long interleaver, it can be assumed that each of these d different bits appears in a different block of Nm bits before mapping to the N-D constellation $\boldsymbol{\Psi}$. Therefore, the binary sequences $\underline{\boldsymbol{c}}$ and $\underline{\check{\boldsymbol{c}}}$ correspond to symbol sequences $\underline{\boldsymbol{S}}$ and $\underline{\check{\boldsymbol{S}}}$, of d N-D signal points $\underline{\boldsymbol{S}} = [\boldsymbol{s}_1, \ldots, \boldsymbol{s}_d]$ and $\underline{\check{\boldsymbol{S}}} = [\check{\boldsymbol{s}}_1, \ldots, \check{\boldsymbol{s}}_d]$. Here, $\boldsymbol{s}_e$ and $\check{\boldsymbol{s}}_e$, $1 \leq e \leq d$, belong to the constellation $\boldsymbol{\Psi}$. With a further assumption that perfect *a priori* information of coded bits fed back from the decoder to the demodulator is achieved, one has the ideal knowledge of the other coded bits carried by the transmitted symbol $\boldsymbol{s}_e$. As a result, only two signal points $\boldsymbol{s}_e$ and $\check{\boldsymbol{s}}_e$ whose labels differ in only 1 bit need to be considered. Then as similar to [7], by using Gaussian probability integral $Q\left(\sqrt{2\gamma}\right) = \frac{1}{\pi}\int_0^{\pi/2} \exp\left(-\frac{\gamma}{\sin^2\theta}\right) \mathrm{d}\theta$, the union bound on $f(d, \boldsymbol{\Psi}, \xi, \boldsymbol{G})$ computed by averaging over all pairs of sequences $\underline{\boldsymbol{S}}$ and $\underline{\check{\boldsymbol{S}}}$ can be simplified to the average over all signal points $\boldsymbol{s}$ and $\boldsymbol{p}$ in the N-D constellation $\boldsymbol{\Psi}$ whose labels differ in only 1 bit at position k, $1 \leq k \leq Nm$, as

$$f(d, \boldsymbol{\Psi}, \xi, \boldsymbol{G}) \leq \frac{1}{\pi}\int_0^{\pi/2} E\left\{\prod_{i=1}^{N}\left(1 + \frac{\|\boldsymbol{g}_i(\boldsymbol{s}-\boldsymbol{p})\|^2}{4N_0 \sin^2\theta}\right)^{-1}\right\}^d \mathrm{d}\theta \tag{4}$$

where

$$\begin{aligned} & E\left\{\prod_{i=1}^{N}\left(1 + \frac{\|\boldsymbol{g}_i(\boldsymbol{s}-\boldsymbol{p})\|^2}{4N_0 \sin^2\theta}\right)^{-1}\right\} \\ = \; & \frac{1}{Nm2^{Nm}} \sum_{\boldsymbol{s}\in\boldsymbol{\Psi}} \sum_{k=1}^{Nm} \left[\prod_{i=1}^{N}\left(1 + \frac{\|\boldsymbol{g}_i(\boldsymbol{s}-\boldsymbol{p})\|^2}{4N_0 \sin^2\theta}\right)^{-1}\right] \end{aligned} \tag{5}$$

and $\boldsymbol{g}_i$ is the ith row of $\boldsymbol{G}$. The single integral in (4) can be efficiently computed and it provides an accurate approximation for the asymptotic performance.

Using the inequality $Q\left(\sqrt{2\gamma}\right) < \frac{1}{2}\exp(-\gamma)$, the function $f(d, \boldsymbol{\Psi}, \xi, \boldsymbol{G})$ can be approximated at high SNR as:

$$f(d, \boldsymbol{\Psi}, \xi, \boldsymbol{G}) \sim \frac{1}{2}\left[\delta(\boldsymbol{\Psi}, \xi, \boldsymbol{G})\right]^d \tag{6}$$

where $\delta(\boldsymbol{\Psi}, \xi, \boldsymbol{G})$ is written as:

$$\delta(\boldsymbol{\Psi}, \xi, \boldsymbol{G}) = \frac{1}{Nm2^{Nm}} \sum_{\boldsymbol{s}\in\boldsymbol{\Psi}} \sum_{k=1}^{Nm} \prod_{i=1}^{N}\left(1 + \frac{\|\boldsymbol{g}_i(\boldsymbol{s}-\boldsymbol{p})\|^2}{4N_0}\right)^{-1} \tag{7}$$

The parameter $\delta(\boldsymbol{\Psi}, \xi, \boldsymbol{G})$ should be made as small as possible to minimize the asymptotic BER. In [7], without using SSD, i.e., $\boldsymbol{G} = \boldsymbol{I}_N$, an algorithm to construct a multi-D mapping that minimizes $\delta(\boldsymbol{\Psi}, \xi, \boldsymbol{I}_N)$ is proposed. This mapping shall be referred to as multi-D anti-Gray mapping.

When SSD is applied, let $\boldsymbol{x}$ and $\boldsymbol{y}$ be the rotated versions of $\boldsymbol{s}$ and $\boldsymbol{p}$, respectively. Observe that with full diversity rotation $\boldsymbol{G}$, each component $\boldsymbol{g}_i(\boldsymbol{s}-\boldsymbol{p}) = x_i - y_i$ is non-zero. Therefore, at high SNR, using the approximation $(1+x)^{-1} \approx x^{-1}$ when $x \to \infty$, $\delta(\boldsymbol{\Psi}, \xi, \boldsymbol{G})$ can be simplified to

$$\delta(\boldsymbol{\Psi}, \xi, \boldsymbol{G}) \approx (4N_0)^N \hat{\delta}(\boldsymbol{\Psi}, \xi, \boldsymbol{G}) \tag{8}$$

where

$$\hat{\delta}(\boldsymbol{\Psi}, \xi, \boldsymbol{G}) = \frac{1}{Nm2^{Nm}} \sum_{\boldsymbol{s}\in\boldsymbol{\Psi}} \sum_{k=1}^{Nm} \prod_{i=1}^{N} \frac{1}{\|x_i - y_i\|^2} \tag{9}$$

Different with the design criterion $\delta(\boldsymbol{\Psi}, \xi, \boldsymbol{G})$, the parameter $\hat{\delta}(\Psi, \xi, \boldsymbol{G})$ above does not depend on SNR and it can be more conveniently used to see the effect of the mapping ξ and rotation $\boldsymbol{G}$ to the asymptotic performance.

REFERENCES

[1] E. Zehavi, "8-PSK trellis codes for a Rayleigh fading channel," *IEEE Trans. Commun.*, vol. 40, pp. 873–883, May 1992.

[2] G. Caire, G. Taricco, and E. Biglieri, "Bit-interleaved coded modulation," *IEEE Trans. Inform. Theory*, vol. 44, pp. 927–946, May 1998.

[3] S. Y. L. Goff, "Bandwidth-efficient turbo coding over Rayleigh fading channels," *International Journal of Communication Systems*, vol. 15, pp. 621–633, 2002.

[4] B. M. Hochwald and S. ten Brink, "Achieving near-capacity on mutiple-antenna channel," *IEEE Trans. Commun.*, vol. 51, pp. 389–399, Mar. 2003.

[5] S. ten Brink, G. Kramer, and A. Ashikhmin, "Design of Low-Density Parity-Check Codes for Modulation and Detection," *IEEE Trans. Commun.*, vol. 52, pp. 670–678, Apr. 2004.

[6] H. Niu, M. Shen, and J. A. Ritcey, "Threshold of LDPC-Coded BICM for Rayleigh Fading," *IEEE Commun. Letters*, vol. 8, pp. 455–457, July 2004.

[7] N. H. Tran and H. H. Nguyen, "Design and performance of BICM-ID systems with hypercube constellations," *IEEE Trans. on Wireless Commun.*, vol. 5, pp. 1169–1179, May 2006.

[8] F. Simoens, H. Wymeersch, H. Bruneel, and M. Moeneclaey, "Multi-dimensional mapping for bit-interleaved coded modulation with BPSK/QPSK signaling," *IEEE Commun. Letters*, vol. 9, May 2005.

[9] N. Gresset, J. Boutros, and L. Brunel, "Multidimensional mappings for iteratively decoded BICM on multiple-antenna channels," *IEEE Trans. Inform. Theory*, vol. 51, pp. 3337–3346, Sept. 2005.

[10] J. Boutros and E. Viterbo, "Signal space diversity: A power and bandwidth efficient diversity technique for the Rayleigh fading channel," *IEEE Trans. Inform. Theory*, vol. 44, pp. 1453–1467, July 1998.

[11] Y. Xin, Z. Wang, and G. B. Giannakis, "Space-time diversity systems based on linear constellation precoding," *IEEE Trans. on Wireless Commun.*, vol. 2, pp. 294–309, Mar. 2003.

[12] N. H. Tran, H. H. Nguyen, and T. Le-Ngoc, "Performance of BICM-ID with signal space diversity," *IEEE Trans. on Wireless Commun.*, vol. 6, pp. 1732–1742, May 2007.

[13] A. G. i Fàbregas and G. Caire, "Multidimensional Coded Modulation in Block-Fading Channels," *IEEE Trans. Inform. Theory*, vol. 54, pp. 2367–2372, May 2008.

[14] S. ten Brink, "Designing iterative decoding schemes with the extrinsic information chart," *AEU Int. J. Electron. Commun*, vol. 54, pp. 389–398, Sept. 2000.

[15] S. Benedetto, D. Divsalar, G. Montorsi, and F. Pollara, "A soft-input soft-output APP module for iterative decoding of concatenated codes," *IEEE Commun. Letters*, vol. 1, pp. 22–24, Jan 1997.

[16] S. ten Brink, "Convergence Behavior of Iteratively Decoded Parallel Concatenated Codes," *IEEE Trans. Commun.*, vol. 49, pp. 1727–1737, Oct. 2001.

[17] J. Hagenauer, "The EXIT Chart - Introduction to extrinsic information transfer in iterative processing," in *12th European Signal Processing Conference (EUSIPCO)*, pp. 1541–1548, 2004.

[18] E. Bayer-Fluckiger, F. Oggier, and E. Viterbo, "New algebraic constructions of rotatated Z^n-lattice constellations for the Rayleigh fading channel," *IEEE Trans. Inform. Theory*, vol. 50, pp. 702–714, Apr. 2004.